Automatic Overvoltage Control of Distributed Energy Resources Supporting Enhanced Energy Exploitation in Low-Voltage Networks

Journal:	*IEEE Transactions on Sustainable Energy*
Manuscript ID	Draft
Manuscript Type:	Transactions
Date Submitted by the Author:	n/a
Complete List of Authors:	Alonso, Augusto; Sao Paulo State University Julio de Mesquita Filho, Group of Automation and Integrated Systems; Norwegian University of Science and Technology, Electric Power Engeneering De Oro Arenas, Luis; Universidade Estadual Paulista Julio de Mesquita Filho Faculdade de Engenharia Campus de Ilha Solteira, Brandao, Danilo; Universidade Federal de Minas Gerais, Department of Electrical Engineering Tedeschi, Elisabetta; Norwegian University of Science and Technology, Department of Electric Power Engineering; University of Trento, Department of Industrial Engineering Marafão, Fernando; Universidade Estadual Paulista, Group of Automation and Integrated Systems
Technical Topic Area :	Grid interaction of sustainable energy sources < Transactions on Sustainable Energy, Energy efficiency < Transactions on Sustainable Energy
Key Words:	Overvoltage, Distributed generation, Energy resources, Active power curtailment, Renewable energy sources, Low-voltage networks, Voltage control

SCHOLARONE™
Manuscripts

Automatic Overvoltage Control of Distributed Energy Resources Supporting Enhanced Energy Exploitation in Low-Voltage Networks

Augusto M. S. Alonso, *Student, IEEE*, Luis De Oro Arenas, Danilo I. Brandao, *Member, IEEE*, Elisabetta Tedeschi, *Senior Member, IEEE*, and Fernando P. Marafao, *Member, IEEE*

***Abstract*-- Large amounts of active power injection by inverter-interfaced distributed energy resources (DER) is a common cause of overvoltage in low-voltage networks. Hence, local active and reactive power control (i.e., Volt/Watt and Volt/VAR, respectively) are adopted to limit voltage rise, leading to active power curtailment. This paper proposes an automatic control strategy to steer non-dispatchable (nd-DER) and dispatchable (d-DER) inverters in low-voltage networks, mitigating overvoltage through local and coordinated Volt/Watt and Volt/VAR functionalities. Active power curtailment is avoided whenever possible. The method does not require *i*) the implementation of optimization algorithms or *ii*) knowledge about line impedance parameters or the location of DERs. The control approach exploits the power flow dispatchability of low-voltage networks comprising one point-of-common coupling with the distribution grid, allowing DERs close to the distribution transformer to also contribute to voltage regulation by only using a low-bandwidth communication link. Simulation results show the flexibilities of the proposed approach and demonstrate that energy exploitation can be increased by up to 25% for the considered scenario in comparison to conventional local Volt/Watt or Volt/VAR schemes. Experimental results based on a laboratory prototype with three inverter-interfaced DERs certify the applicability of the approach to real-life implementations.**

***Index Terms*-- Distributed energy resources, overvoltage, reactive power control, voltage control.**

I. Introduction

INVERTER-INTERFACED renewable energy sources (RESs) and energy storage systems (ESSs), namely distributed energy resources (DERs), have become key players in the actual paradigm of low-voltage (LV) electric networks. Although such DERs bring to reality the appealing perspective of sustainable and decentralized energy generation [1], their ever-growing insertion into the grid brings multiple operational complications [2]. For instance, the maintenance of steady voltage profiles in LV networks becomes difficult since large amounts of decentralized active power injection may cause overvoltage conditions [3]. Concomitantly, for the case of non-dispatchable DERs (nd-DERs) (e.g., PV- and wind-based generators), it is generally desired to fully exploit their intermittent energy generation capabilities to improve their energy efficiency and profitability for their owners [4]. Thus, active power curtailment (APC) is as undesired as overvoltage conditions.

The concepts of local active and reactive power control (i.e., Volt/Watt and Volt/VAR control, respectively) have been consolidated as efficient strategies to tackle overvoltage in LV networks, even considered in standards such as [5]. Nonetheless, although effective and fairly easy to implement, the capability to offer non-coordinated Volt/Watt and Volt/VAR functionalities at each inverter usually causes APC at nd-DERs [6].

Moreover, as found in the literature [4, 7], even when dispatchable DERs (e.g., battery-based ESSs (BESSs)) contribute to mitigating overvoltage by implementing conventional Volt/Watt and/or Volt/VAR actions, the DERs' location may affect their participation [7]. As an example, in LV networks with one point-of-common-coupling (PCC) with the distribution grid [4, 8-10], the DERs placed close to the distribution system transformer (DST) slightly participate in overvoltage control [7]. Thus, even if such DERs present available power capabilities, they are not exploited [7].

Many Volt/Watt and Volt/VAR control methods are found in the literature striving to achieve voltage regulation in LV networks and microgrids with high penetration of nd- and d-DERs. Droop control is one commonly used strategy because of its simplicity of implementation. In [8], the use of the same droop coefficients among DERs is compared to the adoption of different coefficients. It is demonstrated that the former approach makes DERs further downstream on the feeder curtail more power than those close to the DST. On the other hand, APC can be equalized [9] among DERs by the latter approach at the expense of higher energy losses. Ref. [10] presents a distributed method to increase the penetration of PV inverters by combining Volt/Watt and Volt/VAR control with smooth droop functions. The location of DERs and their distance from the DST determine if operation occurs with a power factor close to unity or limited to ±0.90. Thus, [10] is model-based and requires information on line impedances and distances between nodes. Similarly, [11] is model-based, but it uses Kalman filter and PV generation prediction. Two wide-area curtailment schemes are proposed in [4] to increase penetration of nd-DERs while tackling voltage rise according to priorities, such as response speed, voltage levels, and unbalance conditions. However, [4] states that additional coordination actions are needed to improve APC performance.

Optimization approaches have also been extensively used to implemented local or coordinated Volt/Watt and/or Volt/VAR actions. In [12], convex optimization is used to optimize the parameters of linear piecewise Volt/Watt and Volt/VAR functions used on the local control of nd-DERs. Minimum

The authors are grateful to FAPESP (Grants 2017/24652-8, 2016/08645-9, 2019/22304-8), and the NFR (Grant f261735/H30).

APC and near-optimal reactive power injection are achieved by [12]. However, [12] relies on voltage sensitivity factors and PV generation prediction. It disregards d-DERs. The generalized Benders decomposition is adopted along with conic programming relaxation in [13] to formulate an optimization problem for eliminating overvoltage by reactive power control. However, as in [9] and [10], knowledge of the grid parameters is required in most optimization-based strategies, complicating implementation in LV networks of different characteristics. A multi-objective genetic algorithm is used in [7] to provide coordinated Volt/VAR control of nd-DERs, increasing the participation in the reactive power support of inverters close to the DST. Ref. [14] also adopts multi-objective optimization and the sensitivity matrix concept to steer droop-based DERs. The goal in [14] is to minimize APC and control the reactive power absorption of nd-DERs to tackle overvoltage in an LV microgrid. It uses a hierarchical scheme in which the primary layer locally regulates droop curves according to voltage setpoints given by the secondary layer. Genetic algorithms are used in [15] to equalize APC among nd-DERs optimally. Nevertheless, it is worth reinforcing that, besides the lack of model-free features, most optimization methods present significant computational complexity [16], making them difficult to be embedded in DERs' digital processors. Moreover, many strategies do not guarantee optimal global solutions, and formulating objective functions is not trivial.

Hence, having in mind the several advantages mentioned above and disadvantages obtained while exploiting DERs to achieve overvoltage control, the basis of this paper is set.

A. Paper Contributions and Organization

This paper encompasses multiple advantageous features previously found in the literature, integrating them into one control strategy capable of mitigating overvoltages. Such features mainly relate to: *i*) the exploitation of DERs of different natures (i.e., nd- and d-DERs); *ii*) the implementation of local and coordinated steering of inverters offering ancillary services [5]; *iii*) the support to enhanced energy exploitation, avoiding APC whenever possible, without implementing complex optimization algorithms; and *iv*) a generic formulation, which is model-free. In particular, the strategy is suitable for LV radial networks of limited size, comprising a dispatchable PCC with the distribution grid (i.e., as in active distribution networks [9], [13], and LV microgrids [14], [17]).

Considering the above-mentioned scenario and incorporated features (i.e., from *i*) to *iv*)), the contributions of this paper are:

- The development of an automatic strategy that steers DERs based on a centralized control infrastructure, coordinating them to offer Volt/VAR and Volt/Watt actions to tackle overvoltage. In addition, the control over the power dispatchability at the network's PCC [17] is also used as an advantage for overall voltage regulation. To the best of the authors' knowledge, no previous work has investigated incorporating the LV network dispatchability at the PCC into a voltage control strategy.
- The strategy only uses a low-bandwidth communication channel to integrate nd- and d-DERs, also accommodating DERs that do not present communication interface and operate only based on local measurements.
- The strategy reduces APC concerning Volt/Watt and Volt/VAR curves implemented only locally at DERs by combining local and coordinated control actions and allowing Volt/VAR to take precedence over Volt/Watt. Moreover, all DERs contribute to voltage regulation (i.e., even those placed close to the DST).
- Experimental results are presented to validate the feasibility of the overvoltage regulation scheme to real-life applications, unlike in the literature.

A comparative table relating to previous literature works is presented as supplementary material in this paper to support the stated novelties. Finally, this paper is organized as follows. Section II introduces the considered LV network topology and control infrastructure of nd- and d-DERs. The proposed automatic overvoltage control is presented in Section III, and simulation results are brought in Section IV, comprising different operational conditions and comparisons against pure local overvoltage control. Experimental results are shown in Section V, and conclusions are summarized in Section VI.

II. Considered LV Network and Control Layout

The scenario of the LV network herein considered is one of a dynamic electrical system of limited size, comprising several DERs that are interfaced by inverters. Such a scenario relates to LV radial networks presenting a single PCC with the upstream distribution grid. As seen in Fig. 1, the CIGRE's LV European benchmark [18] represents an example of such a network used in this paper as a testbench in Section IV. Note that this testbench encompasses a PCC determined by the placement of the DST. Besides, line impedances of low *X/R* ratio (i.e., < 1) interconnect electric nodes (*B_*), and several inverters modeled as nd- and d-DERs exist. The network parameters are in [18] (see also supplementary material). In Fig. 1, five nd-DERs (i.e., nd-DER_1 to nd-DER_5) are modeled as PV- or wind-based sources, knowing that nd-DER_1 and nd-DER_2 operate without communication. Moreover, three d-DERs (i.e., d-DER_1 to d-DER_3) are modeled as BESSs.

Regarding the control perspective, a central controller (CC) is placed at the PCC to manage the overall operation of the network. Such management occurs based on: *i*) local measurements from active nodes (i.e., the ones where communication-based DERs are connected to); as well as *ii*) utilizing transmitted control coefficients (i.e., $\alpha_{1\parallel}$ and $\alpha_{1\perp}$, explained in Section II-B) that allow d-DERs to contribute to the network's active and reactive current proportionally

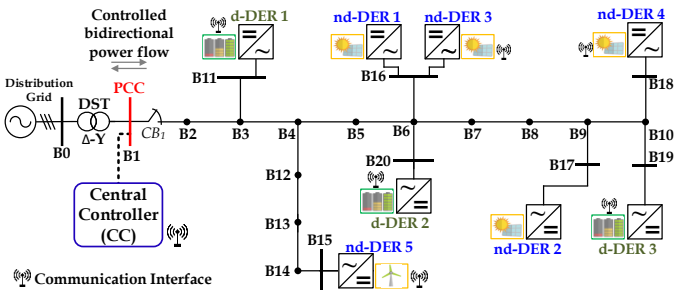

Fig. 1. The layout of the LV network based on the CIGRE benchmark [18].

demands according to different operational goals. Data transmission occurs periodically among the DERs and the CC through a low-bandwidth communication link [19].

The proposed automatic overvoltage mitigation integrates local and coordinated features of DERs, depending on the nature of the operation. For instance, d-DERs are driven by a coordinated control algorithm, providing cooperative Volt/Watt and Volt/VAR actions. In contrast, nd-DERs endowing communication operate under a mixed scheme between local and remote control according to the network operational goals. Lastly, DERs lacking a communication interface operate individually, only based on their local goals. For all DERs in this paper, their inverters are modeled with LCL filters considering active damping as in [20], as shown in Fig. 2. Thus, the overall control features of DERs are explained as follows.

A. Control of Non-Dispatchable DERs

The major goal of nd-DERs is to feed-in active power to the grid. However, ancillary services related to active (i.e., Volt/Watt) and reactive (i.e., Volt/VAR) power control are implemented as specific functions for grid support to avoid local overvoltage conditions. Thus, local Volt/Watt and Volt/VAR curves are implemented at each nd-DER, as shown in Fig. 3-a. Two categories of non-dispatchable inverters are herein considered, ensuring that the proposed control method accommodates various commercial technologies. The first category comprises a communication interface, and the absence of it characterizes the second category.

For the case in which communication is available, remote control is implemented, so the CC partially intervenes in the operational setting. For instance, such nd-DERs present their classic basic control loops (i.e., current, voltage, and/or power loops) embedded in their hardware, but remote control managed by the CC can enable operational functionalities if desired. Additionally, the variable $\gamma_{OV}^{nd\ DER}$ sent from the CC to an nd-DER (see Fig. 2) is responsible for determining which of the voltage control curves is enabled, if needed. Thus, under the occurrence of overvoltage at the point of connection (PoC) of an nd-DER, the CC sends a control signal that enables such inverter to activate its Volt/Watt (i.e., $\gamma_{OV}^{nd\ DER} = 1$) or Volt/VAR (i.e., $\gamma_{OV}^{nd\ DER} = 2$) functionality. Such Volt/Watt and Volt/VAR splines seen in Fig. 3-a are only locally implemented at each nd-DER, and if $\gamma_{OV}^{nd\ DER} = 0$, both are disabled. On the other hand, the nd-DERs not capable of communicating with the CC (i.e., as for the second category) provide active power injection into the network with local Volt/Watt control activated. Thus, nd-DERs without communication always consider $\gamma_{OV}^{nd\ DER} = 1$.

The local Volt/Watt and Volt/VAR controls in Fig. 3-a operate as follows. If the local voltage measurement of an nd-DER exceeds the respective voltage limit ($\bar{V}^{lim}$), the active or reactive power injection performed by that inverter is adjusted to constrain the voltage rise. Concerning the sequence of operation, Volt/Watt control is always set as default for all nd-DERs. However, as discussed in Section III, the CC knows if the communicating nd-DERs operate intending to inject active power at nominal capacity. In case this condition is true, Volt/VAR cannot be offered unless the inverter is designed with additional power margins to be used for this purpose [21]. Thus, Volt/Watt control is maintained by stating $\gamma_{OV}^{nd\ DER} = 1$, inherently leading to the occurrence of APC. On the other hand, if remaining power capability is available, the status of the variable $\gamma_{OV}^{nd\ DER}$ is changed to 2, so Volt/VAR is enabled at that inverter. This approach allows using reactive control as the first measure, consequently avoiding APC.

Lastly, the established thresholds and measurements used for voltage control are calculated according to [5], being the average (AVG) value of the three-phase rms voltages of a PoC or PCC (namely, $\bar{V}$).

B. Control of Dispatchable DERs

In this paper, d-DERs are driven by a coordinated control strategy, namely Generalized Current-Based Control (GCBC) [19], processed at the CC. However, different from [19], herein a novel implementation of the GCBC considers the status of the PoC voltage ($\bar{V}$) of each d-DER (i.e., endowing communication capability) to implement the automatic overvoltage regulation as explained in Section III. Coordinated Volt/Watt and Volt/VAR control of d-DERs is supported by the GCBC, which can regulate the active and reactive power dispatched through the PCC (see Fig. 1) according to voltage responses in the grid. Thus, this novel implementation is explained as follows.

The GCBC is formulated based on the analysis of peak current terms flowing within the LV network (i.e., considering those terms measured by the communicating DERs and the ones seen at the PCC). Coordination of d-DERs occurs utilizing four steps: *i)* local evaluation of electrical quantities; *ii)* GCBC processing at the CC; *iii)* power dispatchability and

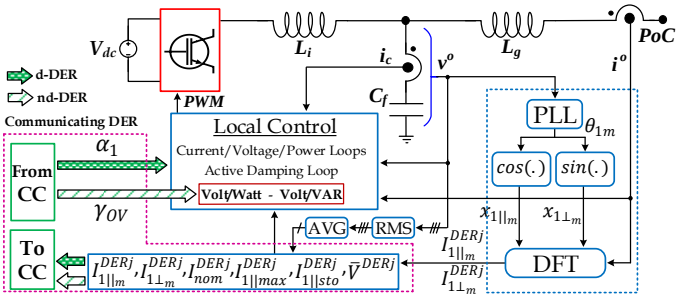

Fig. 2. Single-phase equivalent circuit for the local control of nd- or d-DERs.

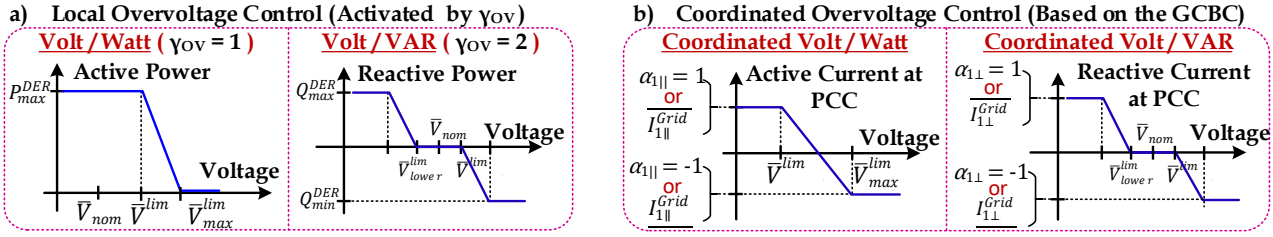

Fig. 3. Volt/Watt and Volt/VAR piecewise functions for: (a) local voltage control at nd-DERs; (b) coordinated voltage control at d-DERs.

coordinated voltage support; and *iv*) local current reference setting. These settings are described in the following.

Let us consider the existence of *J* inverters dispersed over the network. Firstly, the local evaluation of electrical quantities is explained. At each *j*-th d-DER, and at the CC, the output instantaneous current (i_m^o) is used for the detection of the magnitudes (i.e., peak values) of its in-phase (||) and quadrature (⊥) terms, as shown in Fig. 2. Herein, the subscript *m* stands for each phase of the three-phase system (i.e., *m* = *a*, *b*, *c*). Such fundamental component identification of currents is performed by a discrete Fourier transform (DFT) method, thoroughly explained in [19]. For that, unitary in-phase and quadrature signals, $x_{1\|_m}$and $x_{1\perp_m}$, respectively, are attained from the synchronization angle (θ_{1m}) calculated by a phase-locked loop (PLL) algorithm, with the *m*-phase voltage of that PoC (v_m^o). The calculated peak values of active and reactive currents (i.e., from DERs and PCC) use the nomenclature $I_{1\|_m}$ and $I_{1\perp_m}$, respectively. Later, such quantities are periodically transmitted from the communicating DERs to the CC within a data packet, also comprising: *i*) their nominal ratings ($I_{nom_m}^{d\ DERj}$); *ii*) their actual capability to inject active current ($I_{1\|max_m}^{d\ DERj}$); *iii*) the peak current that can be absorbed by their storage system ($I_{1\|sto_m}^{d\ DERj}$); *iv*) as well as their average PoC voltage ($\bar{V}^{d\ DERj}$).

The GCBC processing gives the second step at the CC. The GCBC is implemented as follows at the beginning of a control cycle "*k.*" After acquiring the above-mentioned local electrical quantities from d-DERs, the CC calculates the total (i.e., superscript "*t*") peak currents being processed by the inverters, as in (1). The sum in (1) is also applied to the capabilities $I_{nom_m}^{d\ DERt}$, $I_{1\|max_m}^{d\ DERt}$ and $I_{1\|sto_m}^{d\ DERt}$. It is reinforced that (1) is valid because of the low *X/R* ratio discussed in Section II.

$$I_{1\|_m}^{\mathrm{d}\ DERt}(k) = \sum_{j=1}^{J} I_{1\|_m}^{\mathrm{d}\ DERj}(k) \tag{1.a}$$

$$I_{1\perp_m}^{\mathrm{d}\ DERt}(k) = \sum_{j=1}^{J} I_{1\perp_m}^{\mathrm{d}\ DERj}(k) \tag{1.b}$$

Then, once the CC calculates the currents seen by the upstream grid at PCC, $I_{1\|_m}^{Grid}$ and $I_{1\perp_m}^{Grid}$, it yields to obtain current references, $I_{1\|_m}^{*}$ and $I_{1\perp_m}^{*}$, to be shared by the d-DERs at the next control cycle "*k+1*", as given by (2).

$$I_{1\|_m}^{*}(k+1) = I_{1\|_m}^{Grid}(k) + I_{1\|_m}^{\mathrm{d}\ DERt}(k) - I_{1\|_m}^{Grid*}(k+1) \tag{2.a}$$

$$I_{1\perp_m}^{*}(k+1) = I_{1\perp_m}^{Grid}(k) + I_{1\perp_m}^{\mathrm{d}\ DERt}(k) - I_{1\perp_m}^{Grid*}(k+1) \tag{2.b}$$

When the d-DERs control active power, $I_{1\|_m}^{*}$ is set as the control goal, always complying with $I_{max_m}^{\mathrm{d}\ DERt}$ and $I_{sto_m}^{\mathrm{d}\ DERt}$ whether, respectively, injection or absorption (i.e., storage) is intended. Likewise, $I_{1\perp_m}^{*}$ enables inductive or capacitive reactive current sharing among the d-DERs (i.e., if positive or negative, respectively). Thus, considering the overall peak current capability of the network ($\sqrt{\Delta I_m}$) [19], two scaling coefficients per-phase, given by (3), are calculated by the CC and transmitted to the d-DERs to provide coordinated actions.

$$\alpha_{1\|_m} = \frac{I_{1\|_m}^{*}(k+1)}{\sqrt{\Delta I_m}} \tag{3.a}$$

$$\alpha_{1\perp_m} = \frac{I_{1\perp}^{*}(k+1)}{\sqrt{\Delta I_m}} \tag{3.b}$$

The references $I_{1\|_m}^{Grid*}$ and $I_{1\perp_m}^{Grid*}$ in (2) are the desired peak currents for the PCC in ""*k+1*", which is important for overvoltage control, as explained in the following.

The third step is responsible for the network power dispatchability at PCC and coordinated voltage support. As active and reactive power controllability at the PCC can be inherently achieved utilizing $I_{1\|_m}^{Grid*}$ and $I_{1\perp_m}^{Grid*}$, coordinated Volt/Watt and Volt/VAR are offered by analyzing voltages from the PCC and DERs' PoCs. This functionality occurs if demanded by the automatic overvoltage scheme explained in Section III, as the CC can detect overvoltages within the network when communicating DERs periodically transmit their data packets (i.e., which comprise their average PoC voltage $\bar{V}^{DERj}$). If coordinated Volt/VAR is desired, the reactive current term $I_{1\perp_m}^{Grid*}$ is iteratively adjusted by (4.a), which is used to feed (2). Likewise, $I_{1\|_m}^{Grid*}$ can be adjusted by (4.b) to provide coordinated Volt/Watt. $\delta_{1\|}$ and $\delta_{1\perp}$ are set as constants, ranging from 0 to 1 to regulate the steps of the active and reactive currents dispatched at the PCC at each *k+1* control cycle.

$$I_{1\perp_m}^{Grid*}(k+1) = I_{1\perp_m}^{Grid*}(k) + \delta_{1\perp}.\sqrt{\Delta I_m} \tag{4.a}$$

$$I_{1\|_m}^{Grid*}(k+1) = I_{1\|_m}^{Grid*}(k) + \delta_{1\|}.\sqrt{\Delta I_m} \tag{4.b}$$

It is worth highlighting that such active and reactive power dispatchability at the PCC is, however, constrained to upper ($\overline{I_{1\|_m}^{Grid}}$and $\overline{I_{1\perp_m}^{Grid}}$) and lower ($\underline{I_{1\|_m}^{Grid}}$ and $\underline{I_{1\perp_m}^{Grid}}$) limits given by contractual relations between the network and upstream distribution grid [22]. Hence, the network cannot freely dispatch active and reactive power as desired by its operational manager, is also constrained by the d-DERs power capabilities [23].

Finally, the last step is given by the current setting at d-DERs. To allow the d-DERs to inject the desired currents, their instantaneous *m*-phase current reference (i_m^{j*}) is locally constructed based on the previous steps. Such currents are set according to (5), based on the coefficients (α_1) and the local capability of the *j*-th d-DER [19].

$$i_m^{j*} = \left(\alpha_{1\|_m} \cdot \sqrt{\Delta I_{1\|_m}^{j}}\right) \cdot x_{1\|_m}^{j} + \left(\alpha_{1\|_m} \cdot \sqrt{\Delta I_{1\perp_m}^{j}}\right) \cdot x_{1\perp_m}^{j} \tag{5}$$

III. Automatic Overvoltage Control Strategy

The proposed automatic overvoltage control is summarized in Fig. 4. The main concept behind this approach is to take advantage of the before-mentioned local and coordinated Volt/VAR features of nd- and d-DERs, respectively, in such a way that reactive power control takes precedence over APC whenever it is possible. It is reinforced that this scheme is not applicable to regulate DERs, not endowing communication interface. Nevertheless, such a proposed scheme indirectly affects their nodal operation, reducing local APC.

Let us refer to Fig. 4 to explain the proposed automatic scheme, which is only processed at the CC at the beginning of a control cycle *k*, before initializing the GCBC strategy. As all communicating inverters transmit $\bar{V}^{DERj}$, when an overvoltage occurs, the CC knows which *j*-th DER requires intervention. Thus, if this is an nd-DER that is not injecting active power at the nominal rating, local Volt/VAR is enabled at that DER by

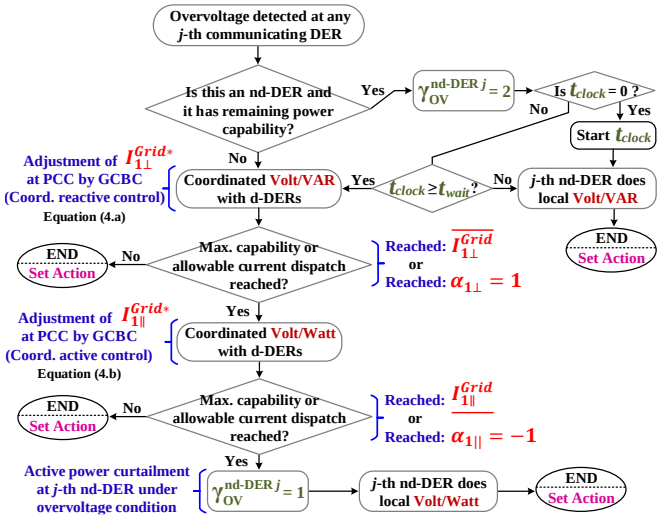

Fig. 4. Proposed scheme for automatic overvoltage control running at the CC.

the CC, by transmitting $\gamma_{OV}^{nd\ DER} = 2$ instead of using the default local Volt/Watt (i.e., $\gamma_{OV}^{nd\ DER} = 1$) that causes APC. If this condition occurs, a timer (t_{clock}) is initiated and a wait time (t_{wait}) is used to consider steady-state accommodation before moving to the next action in Fig. 4. t_{wait} is set according to the network needs (i.e., as for safety and stability reasons) or based on grid codes [5]. Yet, t_{clock} is set to zero when the overvoltage is solved or the next action in Fig. 4 is enabled.

Hence, if the local Volt/VAR control of an nd-DER is either not enabled or not capable of solving the overvoltage issue at that the cycle *k*, d-DERs are cooperatively employed to iteratively increase the dispatch of reactive power through the PCC, according to (4) and based on the GCBC strategy. Consequently, resulting in the coordinated Volt/VAR action seen in Fig. 3-b. In addition, such steering of d-DERs occurs without knowing grid impedances or the inverters' locations. In case of reaching either the maximum reactive (i.e., inductive) current allowed to flow through the PCC ($\underline{I_{1\perp_m}^{Grid}}$) or the overall power capability of d-DERs (i.e., resulting in $\alpha_{1\perp_m} = 1$), such coordinated Volt/VAR feature is constrained.

Although Volt/VAR control is effective, it is proved in the literature that Volt/Watt control is more efficient to mitigate overvoltage in LV networks [8, 12], because of the low *X/R* ratio of line impedances. Hence, when Volt/VAR control cannot be further processed and the overvoltage has not been solved, Fig. 4 demands Volt/Watt to be enabled by iteratively controlling $I_{1\|_m}^{Grid*}(k+1)$. Therefore, proportionally steering d-DERs to absorb power (i.e., the charge of storage systems). This feature can occur until the full state of charge is reached (i.e., $I_{min_m}^{DERt} = 0$; e.g., for battery-based DERs), or the power dispatch limit ($\underline{I_{1\|_m}^{Grid}}$) is reached, or overvoltage is mitigated.

Up to this stage in Fig. 4, APC does not occur at nd-DERs endowing communication. Additionally, the scheme automatically induces communication-free DERs to reduce APC according to the lowering of the grid voltage profile. At last, in case none of the previous actions can maintain voltages below the limit ($\bar{V}^{lim}$), active power can be locally curtailed at communicating nd-DERs by setting $\gamma_{OV}^{nd\ DER} = 1$, allowing local Volt/Watt to be performed, as seen in Fig. 4.

IV. Simulation Results

Simulation results based on MATLAB/Simulink demonstrate the features of the automatic strategy. The LV network is implemented as described in Section II and Fig. 1, considering the same eight three-phase DERs. It is also set that communication is absent for nd-DER$_1$ and nd-DER$_2$. All nd-DERs begin their operation with Volt/Watt control activated as default (i.e., $\gamma_{OV}^{nd\ DERs} = 1$). Yet, d-DER$_2$ operates only injecting active power, with Volt/Watt locally implemented as well. DER's parameters are in Table I.

The grid presents 230V$_{phase}$ at 50 Hz at the secondary side of the DST. Communication between the CC and DERs is emulated to occur once per line period (i.e., 20 ms). Besides, t_{wait} is set to be 0.2 s (i.e., ten fundamental cycles), and the upper threshold that characterizes overvoltage is hypothetically set to $\bar{V}^{lim}$=243.8V for the sake of highlighting the results. The maximum and minimum limits of active and reactive current dispatch at the PCC are initially set to, $\overline{I_{1\|_m}^{Grid}} = \overline{I_{1\perp_m}^{Grid}} = 200\ A$, and $\underline{I_{1\|_m}^{Grid}} = \underline{I_{1\perp_m}^{Grid}} = -200\ A$. A current step of 4% is considered for (4) (i.e., $\delta_{1\perp} = \delta_{1||} = 0.04$). Also, herein, *P*, *Q* and I_{col} respectively stand for the active and reactive powers, and the three-phase collective current (i.e., $I_{col} = ({I_{RMSa}}^2 + {I_{RMSb}}^2 + {I_{RMSc}}^2)^{1/2}$) of a DER or PCC. Yet, the overall network losses are calculated by summing up the power dissipation overall line impedances.

Three main simulation scenarios are considered. The first scenario shows how the strategy operates when nd-DERs and d-DER$_2$ are functioning at nominal capacity injecting *P*, taking into account the above-mentioned current dispatch limitations. In the second scenario, the network's dispatch limit of reactive current is reduced, showing the method's coordinated Volt/VAR and Volt/Watt features. Finally, the last scenario compares the method against pure Volt/Watt and Volt/VAR.

Initially, a result demonstrates how the grid voltages behave if no overvoltage control is considered (i.e., $\gamma_{OV}^{nd\ DERs} = 0$ and $\alpha_{1||_m} = \alpha_{1\perp_m} = 0$). Fig. 5 shows this introductory simulation comprising the following four intervals: *Int. I*) All DERs are idle; *Int. II*) nd-DER$_1$, nd-DER$_4$, nd-DER$_5$, and d-DER$_7$ inject active power at nominal capacity; *Int. III*) nd-DER$_2$ and nd-DER$_3$ also inject nominal active power; *Int. IV*) d-DER$_2$ is disconnected. Yet, d-DER$_1$ and d-DER$_3$ are idle for all intervals. In this result, as DERs inject *P* at full capacity, most of the network nodes operate with voltages significantly above $\bar{V}^{lim}$, reaching up to 251 V (i.e., the worst-case at Interval III).

A. Scenario 1: Full Generation Capability

For this case, the simulations are shown in Fig. 6, and Table II considers the same previous four intervals of operation but now applying the proposed control strategy. Thus, during

TABLE I - DER'S PARAMETERS USED FOR SIMULATION RESULTS.

Parameter	Value
Nominal Powers [nd-DER$_1$, nd-DER$_2$, nd-DER$_3$, nd-DER$_4$, nd-DER$_5$, d-DER$_1$, d-DER$_2$, d-DER$_3$]	[8, 8, 12, 12, 12, 35, 20, 35] kVA
DC bus voltage	750 V$_{dc}$
LCL filter parameters [L_i, C_f, L_g]	[3.5 mH, 2.2 μF, 1.5 mH]

Interval I all DERs are idling, and the voltage profiles are below $\bar{V}^{lim}$. As the nd-DERs inject P at Interval II, the voltages tend to rise and exceed the allowable threshold. As a result, nd-DER$_4$ and d-DER$_2$ tend to curtail P to limit voltage rise (i.e., see I_{col} in Fig. 6 at the beginning of interval II).

However, since DERs inject P at full capability, the automatic scheme in Fig. 4 determines that Volt/VAR cannot be performed locally by the nd-DERs. Consequently, t_{wait} is not required, resulting in the GCBC promptly coordinates d-DER$_1$ and d-DER$_3$ to dispatch inductive currents through the PCC. Since d-DER$_1$ and d-DER$_3$ have the same nominal capabilities, they proportionally share reactive currents so that the grid voltage is maintained below $\bar{V}^{lim}$. Therefore, Q is practically the same for d-DER$_1$ and d-DER$_3$ (see Table II). Moreover, by doing that, the other DERs follow their local Volt/Watt curves and automatically increase their power injections as their PoCs are not under overvoltage anymore. Note that nd-DER$_1$, nd-DER$_4$, and d-DER$_2$ show practically null APC in steady-state during Interval II (see Table II). However, high losses (i.e., 1249 W) over the line impedances inherently occur because of the DER's active power injection.

For Interval III, as nd-DER$_2$ and nd-DER$_3$ are enabled to inject full active power, besides their local APC, nd-DER$_4$ and d-DER$_2$ are also impacted, and they tend to reduce P because of the rise in their PoC voltages. Nonetheless, the automatic scheme also rapidly senses that voltages are exceeding $\bar{V}^{lim}$ Again, so the coordinated Volt/VAR increases the dispatch of Q through d-DER$_1$ and d-DER$_3$. Again, practically no APC occurs since the Volt/VAR control tackles overvoltages at all monitored nodes. Lastly, at t = 2s, d-DER$_2$ is abruptly disconnected from the grid. The approach senses such voltage variation and reduces the d-DERs' reactive currents, maintaining null APC.

B. Scenario 2: Constrained Reactive Power Dispatch

The reactive current dispatch limit is now changed to $\overline{I_{1\perp_m}^{Grid}} = 100\,A$, to demonstrate the concomitant coordinated Volt/VAR and Volt/VAR proposed actions. The results are seen in Fig. 7 and Table II, in which the first two intervals are the same as in Scenario 1 since $\overline{I_{1\perp_m}^{Grid}}$ is still not reached at them. At Interval III, upon the initialization of nd-DER$_2$ and nd-DER$_3$, the scheme in Fig. 4 strives to increase the reactive current dispatch to mitigate overvoltages. However, due to the lower $\overline{I_{1\perp_m}^{Grid}}$ limit, coordinated Volt/VAR is constrained. Since the automatic scheme detects that the actual reactive current dispatch is not enough to limit the voltage rise, coordinated Volt/Watt starts to be performed by d-DER$_1$ and d-DER$_3$. This phenomenon occurs proportionally to their remaining power capabilities and concomitantly to the coordinated Volt/VAR control. Consequently, as both d-DERs store active power (see the negative values of P for d-DER$_1$ and d-DER$_2$ in Table II), the voltages are below $\bar{V}^{lim}$without APC at d-DERs. Also, see in Table II that both d-DERs share similar P and Q.

Thus, this proves that the method can steer DERs without limiting energy generation. It is important to reinforce that, similar to Interval IV in Scenario 1, by disconnecting d-DER$_2$,

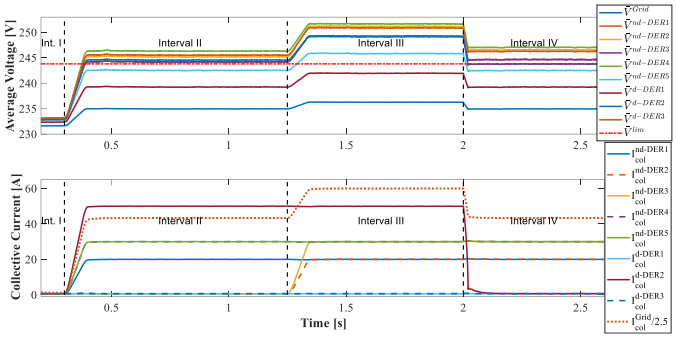

Fig. 5. The operations when all DERs operate injecting power at full capacity and no overvoltage control is implemented. Voltages are measured as $\bar{V}$.

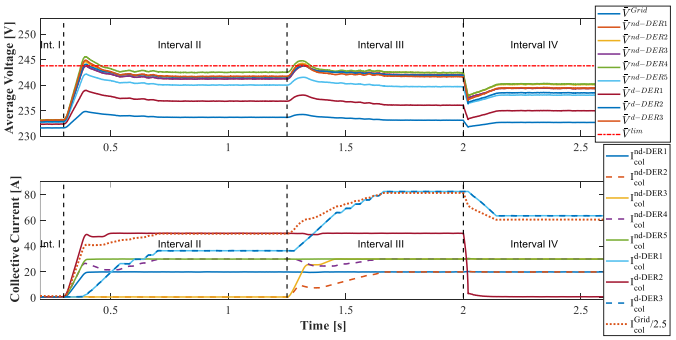

Fig. 6. Simulation results for the proposed approach in Scenario 1.

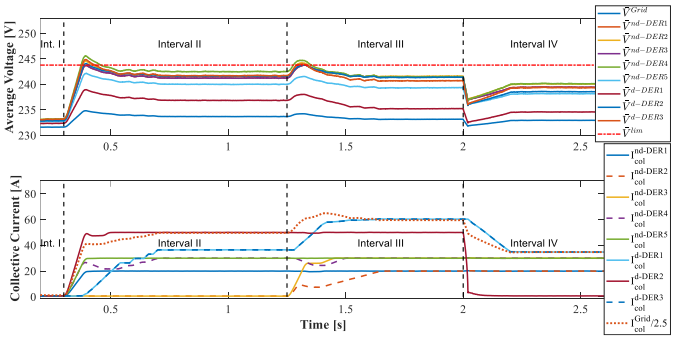

Fig. 7. Simulation results for the proposed approach in Scenario 2.

the Volt/Watt coordination would first reduce the active power absorption of d-DER$_1$ and d-DER$_3$, later reducing their reactive power injection if not needed (see Fig. 4).

C. Brief Comparison to Pure Local Overvoltage Control

Lastly, two simulation cases considering pure Volt/Watt and Volt/VAR control are shown in Figs. 8 and 9 to reinforce the advantages of the proposed scheme in minimizing APC. For these two cases, the same four operational intervals as before are considered, as shown in Figs. 5 and 6. Nonetheless, for the first case, only Volt/Watt is implemented in all DERs. Thus, even d-DER$_1$ and d-DER$_3$ have such pure local control enabled, although they do not inject P into the network (this is done to achieve a fair comparison with Fig. 6).

As shown in Fig. 8 and Table III, such a control method is effective, and voltages are maintained below the given upper threshold for this case. Besides, power losses are significantly lower (i.e., approximately 45%, 78%, and 64% lower for Intervals II, III, and IV) than in *Scenario A* because of the minimized dispatch of P and Q over the grid. The drawback, however, is that most of the DERs operate under APC in all intervals (see Table III). For instance, an overall of 3%,

TABLE II

Steady-state of the simulation results for Scenarios 1 and 2 in Section IV-A and B, respectively. Units: P [W], Q [VAR], I_{col} [A], $\bar{V}$ [V], and Losses [W].

	Scenario 1														**Scenario 2**			
	Int. I		Interval II				Interval III				Interval IV				Interval III			
	P Q	$\bar{V}$	P	Q	I_{col}	$\bar{V}$	P	Q	I_{col}	$\bar{V}$	P	Q	I_{col}	$\bar{V}$	P	Q	I_{col}	$\bar{V}$
PCC	0	231	-51030	16120	149	233	-67180	26060	244	233	-48880	27320	182	232	-52830	24610	179	233
nd-DER$_1$	0	233	8324	0	20	241	8360	91	20	242	8283	87	20	239	8362	87	20	241
nd-DER$_2$	0	233	0	0	0	241	8392	88	20	242	8302	93	20	240	8351	81	20	242
nd-DER$_3$	0	233	0	0	0	241	12560	129	30	242	12430	129	30	239	12540	127	30	241
nd-DER$_4$	0	233	12580	131	30	242	12590	129	30	242	12440	128	30	240	12540	128	30	242
nd-DER$_5$	0	233	12430	125	30	240	12460	134	30	240	12360	121	30	238	12440	130	30	239
d-DER$_1$	0	232	318	7481	36	237	717	16840	82	236	544	12940	63	235	-9008	11450	60	235
d-DER$_2$	0	233	20890	209	50	242	223	20930	50	242	0	0	0	238	20890	210	50	241
d-DER$_3$	0	233	306	7621	36	242	733	17230	82	242	551	13190	63	239	-9211	11700	60	241
Losses	0		1249				3348				1903				2012			

TABLE III

Steady-state simulation results for the local overvoltage control strategies in Section IV-C. Units: P [W], Q [VAR], I_{col} [A], $\bar{V}$ [V], and Losses [W].

	Scenario 3 – Case 1									**Scenario 3 – Case 2**								
	Interval II			Interval III			Interval IV			Interval II			Interval III			Interval IV		
	P	Q	$\bar{V}$	P	Q	$\bar{V}$	P	Q	$\bar{V}$	P	Q	$\bar{V}$	P	Q	$\bar{V}$	P	Q	$\bar{V}$
PCC	-45320	775	234	-46520	813	234	-4423	752	234	-47970	3474	234	-51380	6028	234	-45500	2470	234
nd-DER$_1$	8399	90	242	8328	91	243	8385	95	243	8375	82	243	8398	87	243	8399	89	243
nd-DER$_2$	0	0	243	6277	65	243	6647	72	243	0	0	243	5573	57	243	7149	79	243
nd-DER$_3$	0	0	242	1943	17	243	12590	138	243	0	0	243	2353	27	243	12600	134	243
nd-DER$_4$	9274	97	243	7403	83	243	5651	61	243	8547	91	243	6094	60	243	6537	74	243
nd-DER$_5$	12530	131	241	12560	138	243	12500	137	241	12520	125	241	12530	132	241	12510	132	241
d-DER$_1$	0	0	238	0	0	239	0	0	238	0	0	238	0	0	238	0	0	238
d-DER$_2$	20210	213	243	18810	197	243	0	0	242	20360	214	243	18690	195	243	0	0	242
d-DER$_3$	-3566	42	243	-7216	75	243	-76	0	243	-109	2637	243	-213	5066	243	-81	1680	243
Losses	684			720			674			791			957			730		

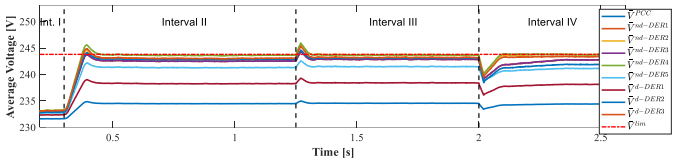

Fig. 8. Operation considering pure local Volt/Watt – Case 1.

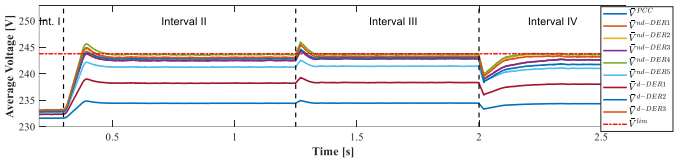

Fig. 9. Operation considering pure local Volt/Watt and Volt/VAR–Case 2.

23% and 11% of APC occurred in the nd-DERs during Intervals II, III, and IV, compared to the automatic scheme. Moreover, since d-DER$_1$ is the closest to the PCC (see Fig. 1), local Volt/Watt makes it idle in all intervals [10], practically not processing (i.e., storing) any active power, as done by d-DER$_3$. This phenomenon does not occur with the proposed strategy, as all d-DERs proportionally tackle overvoltage.

A second simulation case is shown in Fig. 9 to compare with the result in *Scenario A*. Besides the local Volt/Watt implemented at the nd-DERs and d-DER$_2$, pure local Volt/VAR was implemented for d-DER$_1$ and d-DER$_3$. Note in Table III that Q was significantly processed by d-DER$_3$ during all intervals. Consequently, the local control could mitigate overvoltages, but APC still occurred for most of the DERs. The overall APC for nd-DERs was 4%, 25%, and 9% during Intervals II, III, and IV, respectively. Besides, d-DER$_1$ also did not participate in the voltage regulation.

V. Experimental Results

Experiments using a single-phase LV network prototype depicted in Fig. 10-a are shown herein, considering three real inverters (i.e., Inv$_1$, Inv$_2$, and Inv$_3$). They emulate two d-DERs and one nd-DER, with nominal powers of 2.5 and 1.85 kVA, and 2.5 kVA, respectively. The d-DERs present LC output filters (i.e, with 3.5 mH and 2.2 μF), and the nd-DER has an LCL filter (i.e., L_i = 1 mH, C_f = 3.3 μF and L_g = 1 mH). Each DER is fed by a DC voltage source with 270 V$_{dc}$. F28335 DSPs embed the CC and the DER's current controllers, considering sampling and switching frequencies of 12 kHz.

The prototype uses a grid emulator, having a phase voltage of 127 V$_{rms}$ at 60 Hz, with Z_{L1}=2.Z_{L2}=0.18 + j0.188 Ω. DPO3000 oscilloscopes are used for acquiring waveforms, and a digital voltage meter measures the DERs and PCC's voltages. $\bar{V}^{lim}$ was set to be 130V$_{rms}$ for stating overvoltage condition, and d- DERs communicate to the CC each 16 ms. The nd-DER does not participate in the coordinate control, and it operates constantly injecting 950 W without Volt/Watt locally implemented. The results are divided into three intervals: *Int. I*) the only nd- DER$_1$ injects P; *Int. II*) d-DERs begin to mitigate overvoltage according to the proposed strategy; and *Int. III*) a voltage step is applied by the grid, raising the voltage to 133 V$_{rms}$. The rms voltages for the nodes

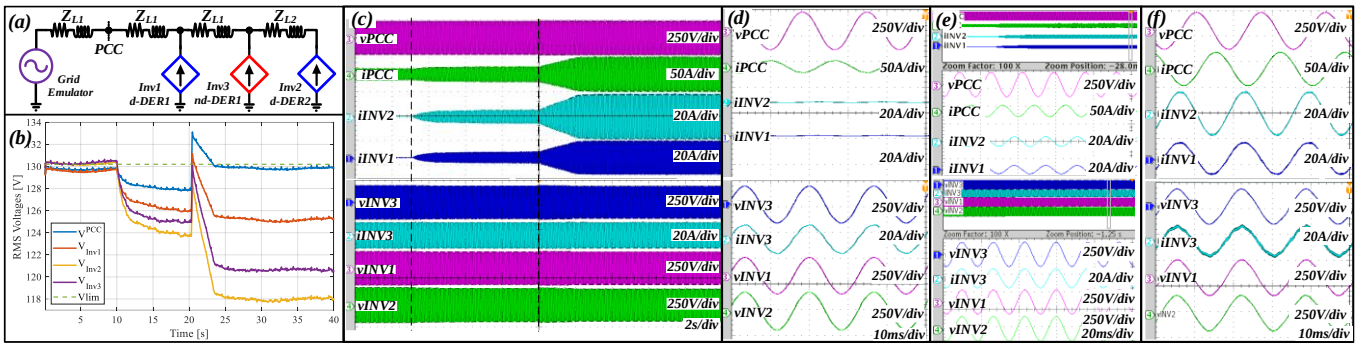

Fig. 10. Experimental results for automatic overvoltage regulation. (a) Circuit of the network used for experiments; (b) rms voltages of the grid nodes comprising inverters; (c) Experimental results of the three intervals tested; (d) Zoom-in-view of Int. I; (e) Zoom-in-view of Int. II; (f) Zoom-in-view of Int. III.

of interest are shown in Fig. 10-b. Yet, the transitions between these stages are in Fig. 10-c, with their zoom-in-views shown in Figs. 11-d, -e, and -f, for intervals I, II, and III, respectively.

Fig. 10-d shows that the PCC current is in-phase with the voltage since nd-DER$_1$ only injects active power, although operating under overvoltage conditions. As the automatic control is enabled, the d-DERs dispatch reactive current through the PCC (see lagging currents in Fig. 10-e) proportionally to their capabilities. Hence, all voltages are found below $\bar{V}^{lim}$. Lastly, as a voltage step is applied to the grid, the approach readjusts the reactive current dispatch until all voltages are again within an acceptable range (see Figs. 10-b, 10-c, and 11-f). The transitions occur smoothly, and no overvoltages/overcurrents occur at the PCC or any DER.

VI. Conclusions

This paper presented a model-free coordination strategy to steer both nd- and d-DERs within an LV network to achieve overvoltage mitigation. It was possible to take advantage of local and coordinated Volt/Watt and Volt/VAR functionalities to avoid APC at nd-DERs utilizing an automatic scheme. Moreover, such a strategy could accommodate DER comprising communication capabilities and those that operate only according to local rules.

Simulation results demonstrated that the method could dynamically steer inverters upon different operation conditions, presenting superior performance (i.e., concerning the minimization of APC) compared to Volt/Watt and Volt/VAR implemented only locally DERs. For the considered simulated cases, the proposed strategy could increase the energy exploitation of nd-DERs by up to 25%. Lastly, experimental results proved that the reactive current dispatch of an LV network could be controlled to mitigate overvoltages, exploiting all DERs, and ensuring that the strategy is suitable for real-life applications. Future work also intends to demonstrate the incorporation of harmonic compensation features into such a voltage control approach.

VII. References

[1] R. S. C. Camargos et al, "Technical and Financial Impacts on Distribution Systems of Integrating Batteries Controlled by Uncoordinated Strategies ," *IEEE Access*, June 2021.

[2] N. K. Roy and H. R. Pota, "Current Status and Issues of Concern for the Integration of Distributed Generation Into Electricity Networks," *IEEE Syst. J.*, vol. 9, Sep. 2015.

[3] R. Tonkoski et al, "Impact of High PV Penetration on Voltage Profiles in Residential Neighborhoods," *IEEE Trans. Sust. Energy*, Jul. 2012.

[4] O. Gagrica et al, "Microinverter Curtailment Strategy for Increasing Photovoltaic Penetration in Low-Voltage Networks," *IEEE Trans. Sust. Energy*, vol. 6, Apr. 2015.

[5] *IEEE Standard 1547 for Interconnection and Interoperability of Distributed Energy Resources with Associated Electric Power Systems Interfaces*, IEEE 1547 Std., 2018.

[6] J. H. Braslavsky, L. D. Collins, J. K. Ward, "Voltage Stability in a Grid-Connected Inverter With Automatic Volt/Watt and Volt/VAR Functions," *IEEE Trans. Smart Grid*, vol. 10, no 1, Jan. 2019.

[7] M. Juamperez, G. Yang, S. B. Kjaer, "Voltage regulation in LV grids by coordinated volt-var control strategies," *J. Mod. Power Syst. Clean Energy*, vol. 4, pp. 319-328, Sep. 2014.

[8] R. Tonkoski et al, "Coordinated Active Power Curtailment of Grid Connected PV Inverters for Overvoltage Prevention," *IEEE Trans. Sust. Energy*, vol. 2, Jul. 2011.

[9] Y. Gerdroodbari et al, "Decentralized Control Strategy to Improve Fairness in Active Power Curtailment of PV Inverters in Low-Voltage Distribution Networks," *IEEE Trans. Sust. Energy*, vol. PP, Jun. 2021.

[10] S. Phkhrem et al, "Enhanced Network Voltage Management Techniques Under the Proliferation of Rooftop Solar PV Installation in LV Distribution Network," *IEEE JESTPE*, vol. 5, no 2, Jun. 2017.

[11] S. Gosh et al, "Distribution Voltage Regulation Through Active Power Curtailment With PV Inverters and Solar Generation Forecasts," *IEEE Trans. Sust. Energy*, vol. 8, Jul. 2017.

[12] S. Weckx et al, "Combined Central and Local Active and Reactive Power Control of PV Inverters," *IEEE Trans. Sust. Energy*, Jul. 2014.

[13] C. Lin et al, "Decentralized Reactive Power Optimization Method for Transmission and Distribution Networks Accommodating Large-Scale DG Integration," *IEEE Trans. Sust. Energy*, vol. 8, Jul. 2017.

[14] T. T. Mai et al, "Coordinated active and reactive power control for overvoltage mitigation in physical LV microgrids," *IET - The J. Engineering*, vol. 2019, no 18, pp. 5007-5011, Aug. 2019.

[15] G. C. Kryonidis et al, "A Coordinated Droop Control Strategy for Overvoltage Mitigation in Active Distribution Networks," *IEEE Trans. Smart Grid*, vol. 8, no 5, pp. 5260-5270, Sep. 2018.

[16] N. Tomin et al, "Voltage/VAR Control and Optimization: AI approach," *IFAC Proceed.*, vol. 51, Dec. 2018.

[17] G. Cravaro et al "A Master/Slave Approach to Power Flow and Overvoltage Control in LV Microgrids," " *Energies*, vol. 12, Jul. 2019.

[18] *Benchmark Systems for Network Integration of Renewable and Distributed Energy Resources*, CIGRE Task Force C6.04.02, 2009.

[19] A. M. S. Alonso et al, "A Selective Harmonic Compensation and Power Control Approach Exploiting Distributed Electronic Converters in Microgrids," " *Int. J. Electr. Power Energy Syst.*, vol. 115, Sep. 2019.

[20] J. P. Bonaldo et al, "Control of 1Φ Power Converters Connected to LV Distorted Power Systems With Variable Comp. Objectives," *IEEE Trans. Power Electron.*, vol. 31, no 3, pp. 2039-2052, Mar. 2016.

[21] Y. Yang et al, "Reactive Power Injection Strategies for 1Φ PV Systems Considering Grid Requirements," *IEEE Trans. Ind. Appl.*, Aug. 2014.

[22] M. F. Zia et al, "MG Transactive Energy: Review, Distributed Ledger Technologies, and Market Analysis," *IEEE Access*, vol. 8, Jan. 2020.

[23] R. A. Fuhrmann et al, "Demand Side Management Strategy for Distribution Networks Volt/Var Control : A FCS-Model Predictive Control Approach," *J. Control Aut. Elec. Syst.*, vol. 31, Aug. 2020.

Supplementary Material

Paper title: Automatic Overvoltage Control of Distributed Energy Resources Supporting Enhanced Energy Exploitation in Low-Voltage Networks

Authors: Augusto M. S. Alonso*, Luis de Oro Arenas, Danilo I. Brandao, Elisabetta Tedeschi, Fernando P. Marafao

*Corresponding author: augusto.alonso@ntnu.no

1) Table IV brings a summarized comparison of the proposed control strategy in this paper with previous works found in the literature.

TABLE IV – LITERATURE REVIEW COMPARISON.

Ref.	Strategy	Model-Free	Volt/Watt	Volt/VAR	Optimal Approach is NOT Needed	Control Power Dispatchability at the Network's PCC	All DERs Participate on Voltage Control	Experimental Results
[4]	Two wide-area APC schemes	✓	✓	✓	✓	✗	✓	✗
[6]	Volt/Watt and Volt/VAR parameter selection with stability robustness	✗	✓	✓	✗	✗	✗	✗
[7]	Coordinated Volt/VAR with genetic algorithm	✓	✗	✓	✗	✗	✓	✗
[8]	Droop control with the same coefficients and with different coefficients	✗	✓	✗	✓	✗	✗	✗
[9]	Decentralized Volt/VAR/Watt control method	✗	✓	✓	✓	✗	✓	✗
[10]	Active and reactive power control methods	✗	✓	✓	✓	✗	✓	✗
[11]	PV gener. forecast and Kalman filter	✓	✓	✓	✓	✗	✗	✗
[12]	Central and local Volt/Watt and Volt/VAR control with convex optimiz.	✗	✓	✓	✗	✗	✓	✗
[13]	Generalized Benders decomposition and conic programming	✗	✗	✓	✗	✗	✗	✗
[14]	Hierarchical control with multi-objective optimiz.	✗	✓	✓	✗	✗	✓	✗
[15]	Coordinated droop control with genetic algorithm	✗	✓	✗	✗	✗	✗	✗
[17]	Master/slave coordination with power-based control	✓	✓	✗	✓	✓	✓	✗
[23]	Model-predictive control and Volt/VAR control	✗	✗	✓	✗	✗	✗	✗
Here	Automatic control - local and coordinated Volt/Watt and Volt/VAR actions and GCBC strategy	✓	✓	✓	✓	✓	✓	✓

2) The line impedance parameters of the testbench adopted for simulations in Section IV are presented in Table V. A complete description of such parameters are found in [18].

TABLE V – LINE IMPEDANCE PARAMETERS OF SIMULATION TESTBENCH.

Node from	Node to	R [Ω/km]	X [Ω/km]	$R_{neutral}$ [Ω/km]	$X_{neutral}$ [Ω/km]	Length [m]
B1	*B2*	0.163	0.136	0.490	0.471	35
B2	*B3*	0.163	0.136	0.490	0.471	35
B3	*B4*	0.163	0.136	0.490	0.471	35
B4	*B5*	0.163	0.136	0.490	0.471	35
B5	*B6*	0.163	0.136	0.490	0.471	35
B6	*B7*	0.163	0.136	0.490	0.471	35
B7	*B8*	0.163	0.136	0.490	0.471	35
B8	*B9*	0.163	0.136	0.490	0.471	35
B9	*B10*	0.163	0.136	0.490	0.471	35
B3	*B11*	1.541	0.206	2.334	1.454	30
B4	*B12*	0.266	0.151	0.733	0.570	35
B12	*B13*	0.266	0.151	0.733	0.570	35
B13	*B14*	0.266	0.151	0.733	0.570	35
B14	*B15*	0.326	0.158	0.860	0.630	30
B6	*B16*	0.569	0.174	1.285	0.865	30
B9	*B17*	1.541	0.206	2.334	1.454	30
B10	*B18*	1.111	0.195	1.926	1.265	30

3) Picture of the single-phase LV network prototype comprising three inverters used for experimental validations.